symmetry

MDPI

Article

# Magnetohydrodynamic (MHD) Flow of Micropolar Fluid with Effects of Viscous Dissipation and Joule Heating Over an Exponential Shrinking Sheet: Triple Solutions and Stability Analysis

**Liaquat Ali Lund [1,2], Zurni Omar [1], Ilyas Khan [3,*], Jawad Raza [4], El-Sayed M. Sherif [5,6] and Asiful H. Seikh [5]**

1 School of Quantitative Sciences, Universiti Utara Malaysia, 06010 Sintok, Kedah; balochliaqatali@gmail.com (L.A.L.); zurni@uum.edu.my (Z.O.)
2 KCAET Khairpur Mirs, Sindh Agriculture University, Tandojam Sindh 70060, Pakistan
3 Faculty of Mathematics and Statistics, Ton Duc Thang University, Ho Chi Minh City 72915, Vietnam
4 Department of Mathematics and Statistics, Institute of Southern Punjab (ISP), Multan 60700, Pakistan; jawad_6890@yahoo.com
5 Centre of Excellence for Research in Engineering Materials, King Saud University, P.O. Box-800, Riyadh 11421, Saudi Arabia; esherif@ksu.edu.sa (E.-S.M.S.); aseikh@ksu.edu.sa (A.H.S.)
6 Electrochemistry and Corrosion Laboratory, Department of Physical Chemistry, National Research Centre, El-Behoth St. 33, Dokki, Cairo 12622, Egypt
* Correspondence: ilyaskhan@tdtu.edu.vn

Received: 3 December 2019; Accepted: 7 January 2020; Published: 10 January 2020


**Abstract:** A numerical study was carried out to examine the magnetohydrodynamic (MHD) flow of micropolar fluid on a shrinking surface in the presence of both Joule heating and viscous dissipation effects. The governing system of non-linear ordinary differential equations (ODEs) was obtained from the system of partial differential equations (PDEs) by employing exponential transformations. The resultant equations were transformed into initial value problems (IVPs) by shooting technique and then solved by the Runge–Kutta (RK) method. The effects of different parameters on velocity, angular velocity, temperature profiles, skin friction coefficient, and Nusselt number were obtained and demonstrated graphically. We observed that multiple solutions occurred in certain assortments of the parameters for suction on a surface. The stability analysis of solutions was performed, and we noted that the first solution was stable while the remaining two solutions were not. The results also showed that the velocity of the fluid increased as the non-Newtonian parameter rose in all solutions. Furthermore, it was detected that the temperature of fluid rose at higher values of the Eckert number in all solutions.

**Keywords:** triple solutions; micropolar fluid; shrinking; stability analysis

## 1. Introduction

The boundary layer flow and heat transfer over a stretching/shrinking sheet have raised extensive interest worldwide, as seen throughout engineering literature, since it has many applications including glass-fiber production, plastic pieces aero-dynamic extrusion, hot rolling, paper production, etc. [1,2]. The micropolar fluid model has attracted more attention from researchers as compared to other non-Newtonian fluid models due to its ability to determine the impacts of local configuration and micro-motions of the fluid components that are disregarded by conventional models [3]. Several operative models have been carefully derived in the steady-state regime. Many researchers considered various non-Newtonian fluid models in their studies. Khan et al. [4] analyzed theoretically

the two-dimensional magnetohydrodynamic (MHD) flow of Eyring–Powell nanofluid over an inclined plane. Jafarimoghaddam [5] investigated the MHD flow of Eyring–Powell fluid in the presence of Darcy–Forchheimer porous medium over the non-linear stretching surface. Kamran et al. [6] concluded that chemical reaction with the Newtonian heating impact is significant in the solidification process of liquid crystals and polymeric suspensions. Beneš et al. [7] investigated the time-dependent flow of an incompressible micropolar fluid through a pipe using asymptotic analysis. Some interesting results of the micropolar fluid are studied in these papers [8–13].

Nowadays, many problems in various fields of industrial and engineering need to be solved due to their important applications in daily life, such as controlling a motor's temperature, machine speed, and constructing bridges and as well as other scientific usages. The model of the micropolar fluid may be utilized to construct the models of the dust or smoke particles in the gas or atmosphere. Unfortunately, these problems or models involve complex non-linear terms which are impossible to solve analytically. There are several methods employed to solve such problems. A well-known method is the shooting method. Lund et al. [14] studied numerically the characteristics of magnetohydrodynamic Casson fluid using shooting and Runge–Kutta numerical algorithms. It was found that the velocity decreases by increasing the Casson parameter in both solutions. Aurangzaib et al. [15] stated that the velocity drops in the first solution when the material parameter is increased, whereas the thickness of the momentum boundary layer increases in the second solution. However, the effects of material parameter are inversely proportional to fluid temperature. Lund et al. [16] extended the work of Aurangzaib et al. [15] for micropolar nanofluid and found three local similarity solutions using shooting method. Further, they also used another numerical method, three-stage Lobatto IIIA formula, to perform analysis of the stability of the solutions. MHD flow of nanofluid over the disk surface was solved by the shooting method [17]. The shooting method is a more appropriate method as compared to other methods to predict more than one solution. Some other interesting works of multiple solutions can be found in these articles [18–23].

Most engineering problems and phenomena of nature need analysis of MHD. It is a fact that the magnetic field exists everywhere in this world which implies that MHD characteristics exist under the availability of conducting fluids in natural phenomena. This phenomenon of MHD is significant in astronomy since most parts of the universe are occupied with spaced, charged particles infused by magnetic fields. Geophysics encounter MHD phenomena when dealing with the presence of conducting fluids and magnetic fields in and around the earth. Furthermore, MHD has great impacts on engineering due to its vital principles. These principles are also applied in numerous industrial applications such as MHD pumps, generators, nuclear reactors cooling, flow meters, heat exchangers, nuclear waste disposal, geothermal energy extractors, and space vehicle impulsion. The presence of a magnetic effect produces a Lorentz force generated by the magnetic field which usually repels the hydrodynamic field in the presence or absence of the permeable matrix. However, the opposite result is observed in the case of angular momentum [24]. Increasing the intensity of the magnetic field leads to greater Lorentz force and therefore skin friction increased [25]. On the other hand, Reddy et al. [26] noticed that the coefficient of skin friction declines with rising values of local Deborah number and magnetic parameter. Pal [27] reported that the impact of augmenting chemical reaction leads to a reduction in the skin friction coefficient at the wall, whereas the reverse behavior is noted by rising the permeability parameter of the porous medium.

To deal with the impact of viscous dissipation is very difficult due to its non-linearity behavior but it is also an important factor in heat transfer. Many researchers have tried to consider this in their studies [28–32]. Lund et al. [33] considered a viscous incompressible electrically-conducting Casson nanofluid over a shrinking sheet and found dual solutions. Further, it is noticed that viscous dissipation improves the flow and temperature of the nanofluid. Adegbie et al. [34] studied a two-dimensional boundary layer flow of micropolar fluid towards a stagnation point over a horizontal linearly stretching surface. Thus, the prime objectives of this study are as follows

1. To extend the problem of Aurangzaib et al. [15] by considering the effect of magnetic, viscous, and Joule heating functions.
2. To find the maximum number of the multiple solutions.
3. To perform stability analysis of multiple solutions in order to determine a stable solution.

To the best of our knowledge, no such model has been considered for multiple solutions. Therefore, these results are new and would provide a good understanding of micropolar fluid.

## 2. Mathematical Formulation

A two-dimensional, laminar boundary layer electrically-conducting incompressible micropolar fluid flow with viscous dissipation along an exponentially shrinking surface is considered. The $u$, $v$ are velocity components corresponding the directions $x$ and $y$, respectively. The $x$-axis is with the surface of the sheet while the $y$-axis is perpendicular to it. Physical model of the problem is shown in Figure 1. According to the above-mentioned assumptions, along with boundary layer approximations, the concerned boundary layer equations of motion along with angular momentum and heat transfer can be written as [15,35]:

$$\frac{\partial u}{\partial x} + \frac{\partial v}{\partial y} = 0 \tag{1}$$

$$u\,\frac{\partial u}{\partial x} + v\,\frac{\partial u}{\partial y} = \left(\vartheta + \frac{\kappa}{\rho}\right)\frac{\partial^2 u}{\partial y^2} + \frac{\kappa}{\rho}\frac{\partial N}{\partial y} - \frac{\sigma B^2 u}{\rho} \tag{2}$$

$$u\frac{\partial N}{\partial x} + v\frac{\partial N}{\partial y} = \frac{\gamma}{\rho j}\frac{\partial^2 N}{\partial y^2} - \frac{\kappa}{\rho j}\left(2N + \frac{\partial u}{\partial y}\right) \tag{3}$$

$$u\,\frac{\partial T}{\partial x} + v\,\frac{\partial T}{\partial y} = \alpha\,\frac{\partial^2 T}{\partial y^2} + \frac{(\mu+\kappa)}{\rho C_p}\left(\frac{\partial u}{\partial y}\right)^2 + \frac{\sigma B^2}{\rho}u^2 \tag{4}$$

Subject to these boundary conditions

$$\begin{cases} v = -v_w(x); \quad u = u_w(x); \quad N = -m\frac{\partial u}{\partial y}; \quad T = T_w(x); \quad at \quad y = 0 \\ u \to 0; \; N \to 0; \quad T \to T_\infty \;\; as \;\; y \to \infty \end{cases} \tag{5}$$

where $\eta$ is the similarity variable, $f(\eta)$ is non-dimensional form of the stream function, and $\theta(\eta)$ denotes the non-dimensional temperature whereas, prime stands for differentiation with respect to variable $\eta$.

The following exponential form of the similarity transformations are used [15],

$$\begin{cases} u = U_w e^{\frac{x}{l}} f'(\eta); v = -\sqrt{\frac{\vartheta U_w}{2l}} e^{\frac{x}{2l}}(f(\eta) + \eta f'(\eta)) N = U_w e^{\frac{3x}{2l}} \sqrt{\frac{U_w}{2\vartheta l}} g(\eta) \\ \theta(\eta) = {}^{(T-T_\infty)}/_{(T_w - T_\infty)}; \; \eta = y\sqrt{\frac{U_w}{2\vartheta l}}\, e^{\frac{x}{2l}} \end{cases} \tag{6}$$

By using Equation (6) in order to transform Equations (1)–(4) in the system of non-dimensional ordinary differential equations, we have

$$f''' + \frac{1}{(1+K)}\left(ff'' - 2f'^2 - Mf'\right) + \frac{K}{(1+K)}g' = 0 \tag{7}$$

$$\left(1 + \frac{K}{2}\right)g'' + fg' - 3gf' - 2Kg - Kf'' = 0 \tag{8}$$

$$\frac{1}{Pr}\theta'' + f\theta' - f'\theta + Ec(1+K)f''^2 + EcMf'^2 = 0 \tag{9}$$

and boundary conditions will be as

$$\begin{cases} f(0) = S;\ f'(0) = -1;\ g(0) = -mf''(0);\ \theta(0) = 1 \\ f'(\eta) \to 0;\ g(\eta) \to 0;\ \theta(\eta) \to 0;\ as\ \eta \to \infty \end{cases} \tag{10}$$

Here, $'$ prime indicates differentiation due to $\eta$, $K = \frac{\kappa}{\mu}$ is the micropolar parameter (non-dimensional material parameter), we assume that $\gamma$ is the given by

$$\gamma = \left(\mu + \frac{\kappa}{2}\right)j = \mu\left(1 + \frac{K}{2}\right)j \tag{11}$$

where $j = \frac{2LVe^{\frac{-x}{l}}}{U_w}$ [15]. Further, $M = \frac{2l\sigma(B_0)^2}{\rho U_w}$ is the magnetic field parameter, $Pr = \frac{\vartheta}{\alpha}$ indicates Prandtl number, $Ec = \frac{U_w^2}{c_p T_0}$ is the Eckert number, and $S$ is the suction/injection parameter. The coefficient of skin friction, local couple stress, and Nusselt numbers is obtained in dimensionless form as

$$C_f(Re_x)^{\frac{1}{2}}\sqrt{\frac{2l}{x}} = (1 + (1-m)K)f''(0); M_x Re_x = \left(1 + \frac{K}{2}\right)g'(0);\ N_u(Re_x)^{-\frac{1}{2}} = -\theta'(0)$$

where $Re_x$ is the Reynolds number.

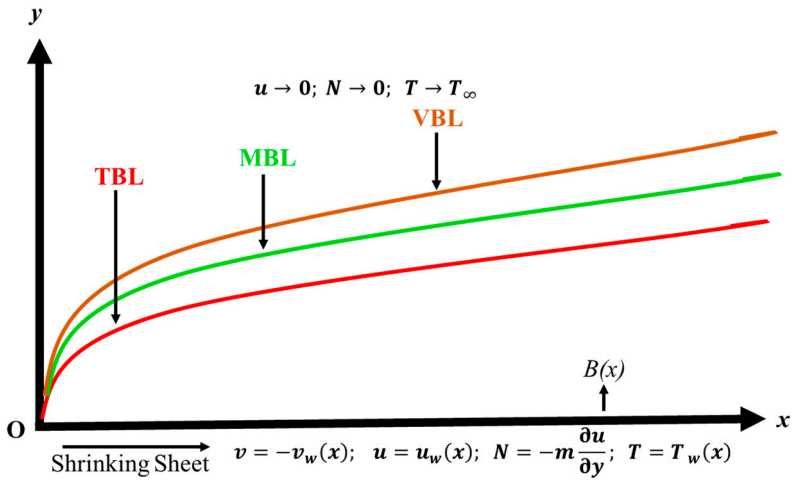


**Figure 1.** Geometry of flow and coordinate system.

## 3. Stability Analysis

In this paper triple solutions were found. When there exists more than one solution, it is necessary to conduct the analysis of stability of solutions in order to indicate the stable solution. According to Usama et al. [36] and Lund et al. [37], the first step of performing stability analysis is to change the governing equations in unsteady flow form by introducing a new similarity variable, $\tau = \frac{U_w}{2l}e^{\frac{x}{l}}.t$.

The new governing equations become

$$\frac{\partial u}{\partial t} + u\frac{\partial u}{\partial x} + v\frac{\partial u}{\partial y} = \left(\vartheta + \frac{\kappa}{\rho}\right)\frac{\partial^2 u}{\partial y^2} + \frac{\kappa}{\rho}\frac{\partial N}{\partial y} - \frac{\sigma B^2 u}{\rho} \tag{12}$$

$$\frac{\partial N}{\partial t} + u\frac{\partial N}{\partial x} + v\frac{\partial N}{\partial y} = \frac{\gamma}{\rho j}\frac{\partial^2 N}{\partial y^2} - \frac{\kappa}{\rho j}\left(2N + \frac{\partial u}{\partial y}\right) \tag{13}$$

$$\frac{\partial T}{\partial t} + u\frac{\partial T}{\partial x} + v\frac{\partial T}{\partial y} = \alpha\frac{\partial^2 T}{\partial y^2} + \frac{(\mu + \kappa)}{\rho C_p}\left(\frac{\partial u}{\partial y}\right)^2 + \frac{\sigma B^2}{\rho}u^2 \tag{14}$$

where $t$ is the time. The similarity variables in Equation (6) with $\tau$ can be written as

$$\begin{cases} \psi = \sqrt{2\vartheta l U_w} e^{\frac{x}{2l}} f(\eta,\tau);\ N = U_w e^{\frac{3x}{2l}} \sqrt{\frac{U_w}{2\vartheta l}} g(\eta,\tau) \\ \theta(\eta,\tau) = {}^{(T-T_\infty)}/_{(T_w-T_\infty)};\ \tau = \frac{U_w}{2l} e^{\frac{x}{l}}.t\ ;\eta = y\sqrt{\frac{U_w}{2\vartheta l}}\, e^{\frac{x}{2l}} \end{cases} \tag{15}$$

By substituting Equation (15) into Equations (12)–(14), we get

$$(1+K)\frac{\partial^3 f(\eta,\tau)}{\partial\eta^3} + f(\eta,\tau)\frac{\partial^2 f(\eta,\tau)}{\partial\eta^2} + K\frac{\partial g(\eta,\tau)}{\partial\eta} - 2\left(\frac{\partial f(\eta,\tau)}{\partial\eta}\right)^2 - M\frac{\partial f(\eta,\tau)}{\partial\eta} - \frac{\partial^2 f(\eta,\tau)}{\partial\tau\partial\eta} = 0 \tag{16}$$

$$\left(1+\frac{K}{2}\right)\frac{\partial^2 g(\eta,\tau)}{\partial\eta^2} + f(\eta,\tau)\frac{\partial g(\eta,\tau)}{\partial\eta} - 3g(\eta,\tau)\frac{\partial f(\eta,\tau)}{\partial\eta} - 2Kg(\eta,\tau) - K\frac{\partial^2 f(\eta,\tau)}{\partial\eta^2} - \frac{\partial g(\eta,\tau)}{\partial\tau} = 0 \tag{17}$$

$$\frac{1}{Pr}\frac{\partial^2\theta(\eta,\tau)}{\partial\eta^2} + f(\eta,\tau)\frac{\partial\theta(\eta,\tau)}{\partial\eta} - \theta(\eta,\tau)\frac{\partial f(\eta,\tau)}{\partial\eta} + Ec(1+K)\left(\frac{\partial^2 f(\eta,\tau)}{\partial\eta^2}\right)^2 + EcM\left(\frac{\partial f(\eta,\tau)}{\partial\eta}\right)^2 - \frac{\partial\theta(\eta,\tau)}{\partial\tau} = 0 \tag{18}$$

Subject to boundary conditions

$$\begin{cases} f(0,\tau) = S;\ \frac{\partial f(0,\tau)}{\partial\eta} = -1;\ \ g(0,\tau) = -m\frac{\partial^2 f(0,\tau)}{\partial\eta^2};\ \theta(0,\tau) = 1 \\ \frac{\partial f(\eta,\tau)}{\partial\eta} \to 0;\ g(\eta,\tau) \to 0;\ \theta(\eta,\tau) \to 0; \qquad as\ \eta \to \infty \end{cases} \tag{19}$$

In order to indicate the solution stability of $f(\eta) = f_0(\eta)$, $g(\eta) = g_0(\eta)$, and $\theta(\eta) = \theta_0(\eta)$ which satisfies the equation of boundary value problem in Equations (16)–(19). For this purpose, we follow the suggestion of Rehman et al. [38] by introducing the following functions:

$$\begin{cases} f(\eta,\tau) = f_0(\eta) + e^{-\varepsilon\tau}F(\eta,\tau) \\ g(\eta,\tau) = g_0(\eta) + e^{-\varepsilon\tau}G(\eta,\tau) \\ \theta(\eta,\tau) = \theta_0(\eta) + e^{-\varepsilon\tau}H(\eta,\tau) \end{cases} \tag{20}$$

where $\varepsilon$ is the unknown eigenvalue which is needed to determine, $F(\eta,\tau)$, $G(\eta,\tau)$, and $H(\eta,\tau)$ which are the small relatives of $f_0(\eta)$, $g_0(\eta)$, and $\theta_0(\eta)$, respectively. Further, Equation (20) is submitted to Equations (16)–(19) by keeping $\tau = 0$, we get

$$(1+K)F_0''' + f_0F_0'' + F_0f_0'' + KG_0' - 4f_0'F_0' - MF_0' + \varepsilon F_0' = 0 \tag{21}$$

$$\left(1+\frac{K}{2}\right)G_0'' + f_0G_0' + F_0g_0' - 3g_0F_0' - 3g_0F_0' - 2K\delta G_0 - K\delta F_0'' + \varepsilon G_0 = 0 \tag{22}$$

$$\frac{1}{Pr}H_0'' + f_0H_0' + F_0\theta_0' - f_0'H_0 - F_0'\theta_0 + 2Ec(1+K)f_0''F''_0 + 2EcMf_0'F_0' + \varepsilon H_0 = 0 \tag{23}$$

Subject to boundary conditions

$$\begin{cases} F_0(0) = 0, \quad F_0'(0) = 0, \quad G_0(0) = -mF_0''(0), \quad H_0(0) = 0 \\ F_0'(\eta) \to 0, \quad G_0(\eta) \to 0, \quad H_0(\eta) \to 0, \quad as\ \ \eta \to \infty \end{cases} \tag{24}$$

It is necessary to determine the initial growth of decay and the initial growth of disturbance of the values of the smallest eigenvalue. In order to find the initial growth of decay and disturbance of the eigenvalue, we have to relax one boundary condition as suggested by Haris et al. [39] and Lund et al. [40]. Physically, this relaxation in boundary condition provides the results of the smallest eigenvalue without loss of generality [41]. Mathematically, it is the step of the algorithm of the stability analysis. In this study, we relaxed the $F_0'(\eta) \to 0$ as $\eta \to \infty$ into $F_0''(0) = 1$.

## 4. Results and Discussion

In this study, the MHD flow of micropolar fluid on an exponentially shrinking surface was investigated. The governing dimensionless equations are solved numerically using the shooting method and multiple solutions are obtained. The comparison of skin friction with the existing work is presented in Figure 2 for the same values of $K$ and $m$. Both solutions show the same critical values at parameter $S$. These dual solutions only exist for certain values of $S_c$. At $S = S_c$, both solutions meet each other. Beyond this critical value, no similarity solution exists as the boundary layer separates from the sheet. The variation of the shear stress with the parameter $S$ is depicted in Figure 3 for various values of micropolar parameter $K$. As anticipated, in the first solution, the shear stress rises with all values of $S$ and declines with $K$. This increment in the shear stress is due to the high values of suction since suction produces more resistance in the fluid flow. Yet, for the second and third solutions, the shear stress reduces with increasing $S$ and has dual solutions at $S_{c1} = 2.1255$ and $S_{c2} = 2.67528$, respectively corresponding to $K = 0.1$ and $K = 0.2$. The variation of the couple stress coefficient with $S$ is depicted in Figure 4 for different values of $K$. This variation is found to be negligible in the first solution, whereas the couple stress coefficient decreases (increases) with an increase in $S$ ($K$) in the second solution. Physically, this is due to the fact that the material parameter supports the particles of the skew-symmetric of the fluid and therefore the couple stress coefficient increases in the second solution. In the third solution, the variation of the couple stress coefficient is totally different. It increases with $S$ and decreases with $K$. Like shear stress, the dimensionless heat transfer coefficient shows the dual nature at the same critical points (Figure 5). All other parameters are kept constant. The first solution for the dimensionless heat transfer coefficient also shows the same nature as the first solution for shear stress. Moreover, heat transfer enhances in the first and second solutions for the high values of mass suctions.

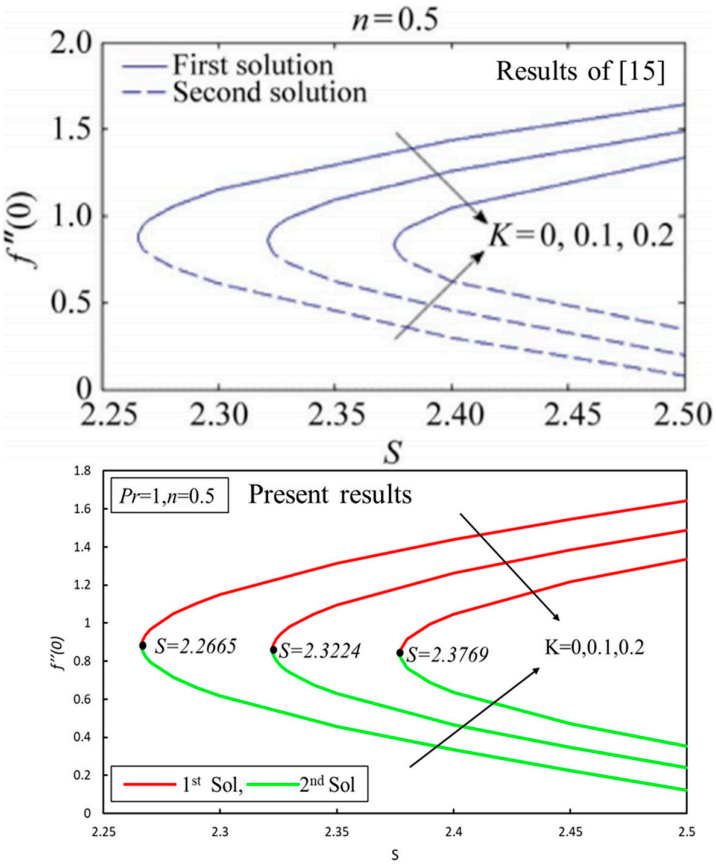


**Figure 2.** Comparison of skin friction coefficient $f''(0)$ at the various values of $S$ for different values of $K$ with Aurangzaib et al. [15].

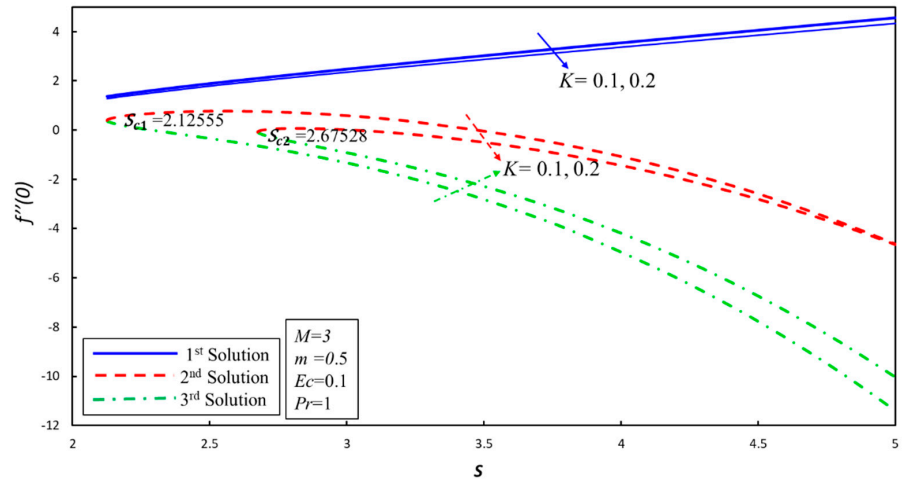


**Figure 3.** The skin friction coefficient $f''(0)$ at various values of $S$ for different values of $K$.

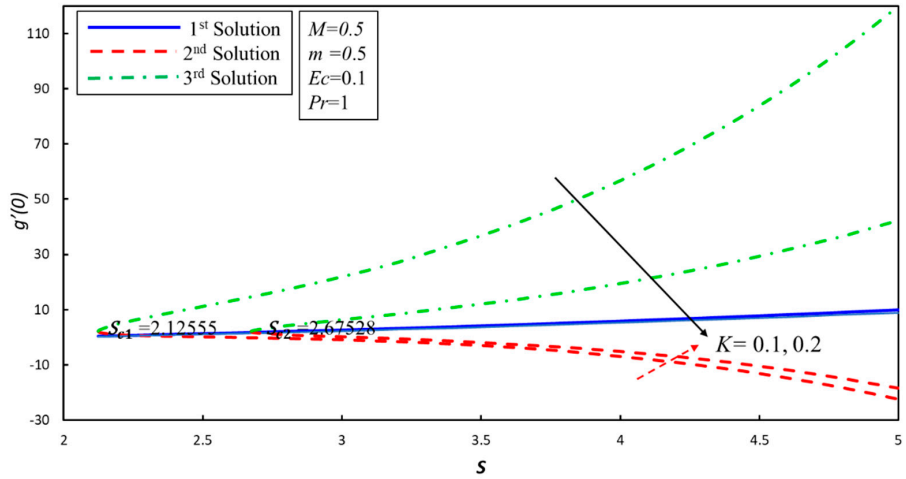


**Figure 4.** The couple stress coefficient $g'(0)$ at various values of $S$ for different values of $K$.

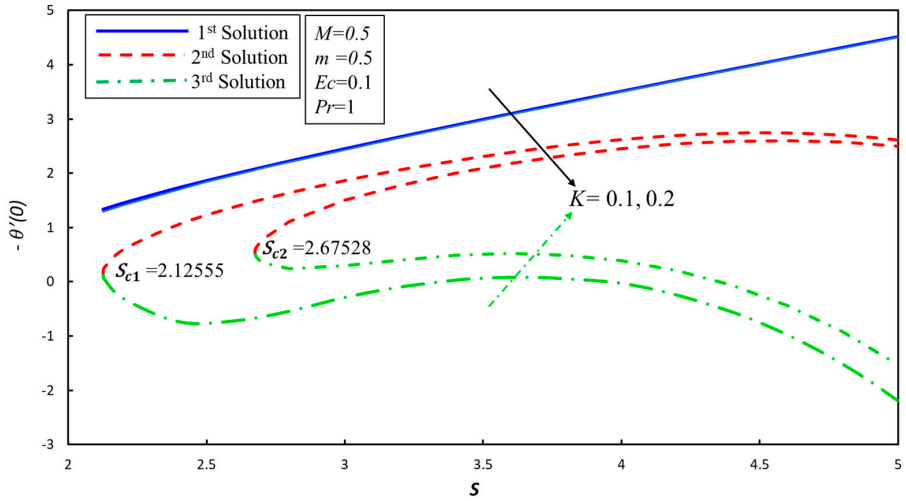


**Figure 5.** The heat transfer coefficient $-\theta'(0)$ along $S$ for different values of $K$.

The velocity profiles of the micropolar fluid for the pertinent parameters are presented in Figures 6–8. Figure 6 illustrates the multiple solutions of the dimensionless velocity for several values of $M$. The remaining parameters are kept constant. It is important to note that these solutions satisfy both boundary conditions. When the intensity of the magnetic field is enlarged, the Lorentz force

increases and thus, the velocity decreases in the first solution. Physically, this reduction in the thickness of the momentum boundary layer is due to the high resistant which is created by the Lorentz force. The dimensionless velocity increases when the effect of the magnetic field is enhanced in both the second and third solutions. The figure also displays that the hydrodynamic boundary layer thickness increases in the second and third solutions. Similarly, the effects of micropolar and slip parameters on the variation of the dimensionless velocity are depicted in Figures 7 and 8, respectively. In each case, three solutions are obtained. It is observed that the velocity of the fluid and its thickness of boundary increases for the higher values of micropolar parameter in all solutions (Figure 7). Physically, this enhancement in the thickness of the momentum boundary layer indicates that the micropolar parameter produces less drag force in the boundary layer separation, while the velocity profiles reduce as the slip parameter enhances (Figure 8), as expected. In each case, the boundary layer thickness is higher in the second and third solutions. This reduction is due to the existence of the singularities in the profiles of the velocity.

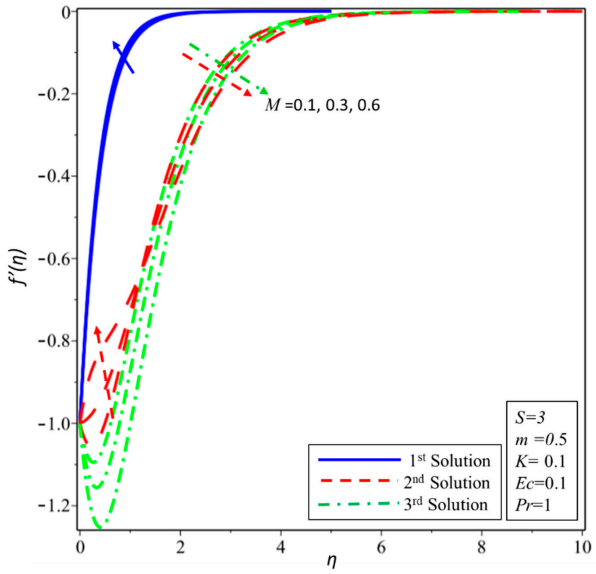


**Figure 6.** Velocity profile for different values of *M*.

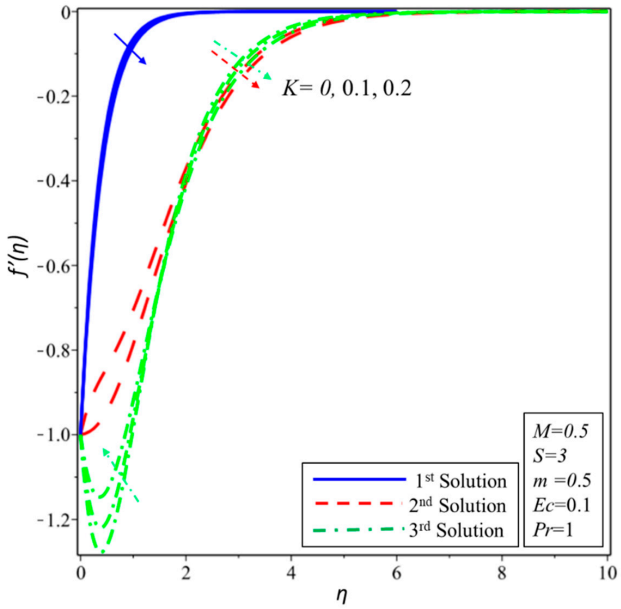


**Figure 7.** Velocity profile for different values of *K*.

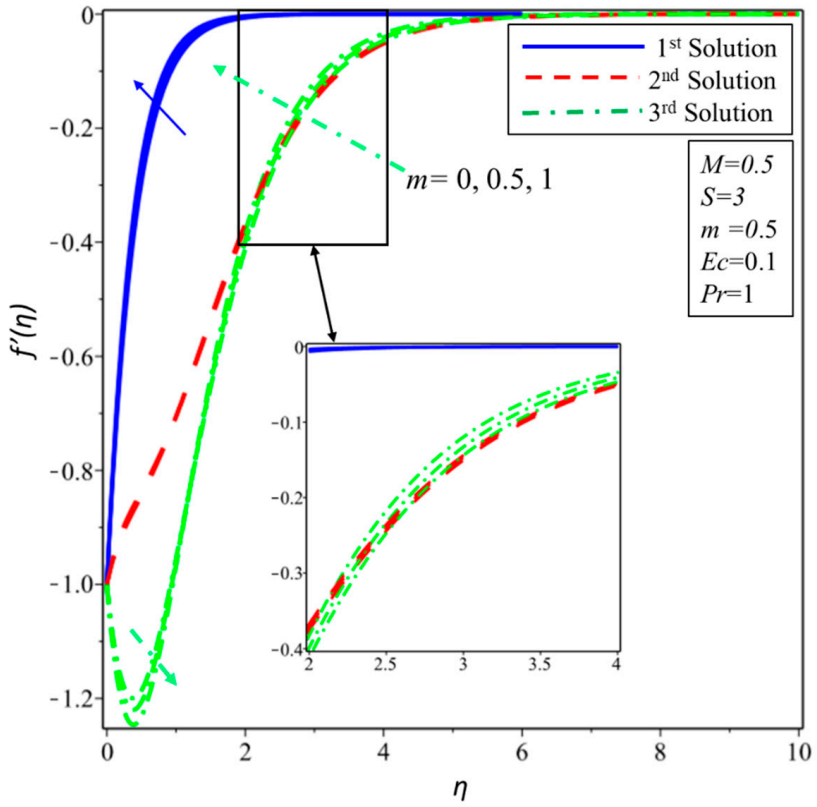


**Figure 8.** Velocity profile for different values of $m$.

The variation in the dimensionless angular velocity with the corresponding micropolar and slip parameters are depicted in Figures 9 and 10. In each case, three solutions are obtained, except $K = 0$. In the first solution, the dimensionless angular velocity increases asymptotically and satisfies the far-field boundary conditions when $K$ and $m$ are increased. In the second solution, the angular velocity rises initially and then declines. The angular velocity decreases with an increase in the micropolar parameter. In the third solution, the angular velocity decreases to a minimum value and then increases to attain the far-field boundary conditions.

The variation of the temperature profiles inside the thickness of the thermal layer for different values of magnetic field $M$, micropolar fluid parameter $K$, Eckert number $Ec$, and Prandtl numbers $Pr$ are revealed in Figures 11–14, respectively. In each case, multiple solutions are investigated. Figure 11 reveals that the first solution is the real possible solution and there is small variation in the profile of velocity. In the second (third) solution, the dimensionless temperature decreases (increases) with the magnetic field. The increment in the temperature of the fluid is expected when the magnetic field increases but the interesting scenario happens in the second solution. The reduction in the profile of temperature in the second solution is due to the fact that the Lorentz force does not produce the resistance which is expected for the higher value of $M$. Similar behavior for the dimensionless temperature against different values of K can be observed in Figure 12. The Eckert number describes heat dissipation within the thermal boundary layer. It is also noticed that when $K = 0$ there are two solutions only. Further, as the Eckert number increases, the heat dissipation increases and consequently, the dimensionless temperature increases (Figure 13). Physically, it can be explained that the thermal boundary layer thickness increases for the intense impact of kinetic energy which is created for higher values of the Eckert number, as a result, profiles of temperature and thickness of the thermal boundary layer enhance. Figure 14 explains the variation of the dimensionless temperature with the Prandtl number. As the Prandtl number increases, the thermal resistance increases and consequently, the dimensionless temperature decreases, and the momentum diffusivity dominates the behavior.

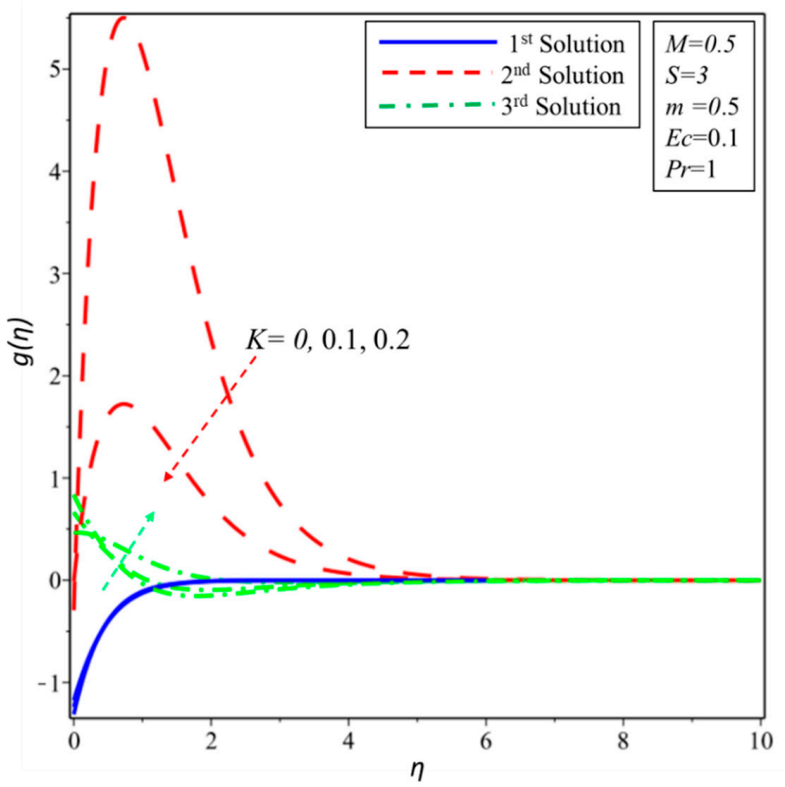


**Figure 9.** Angular velocity profile for different values of *K*.

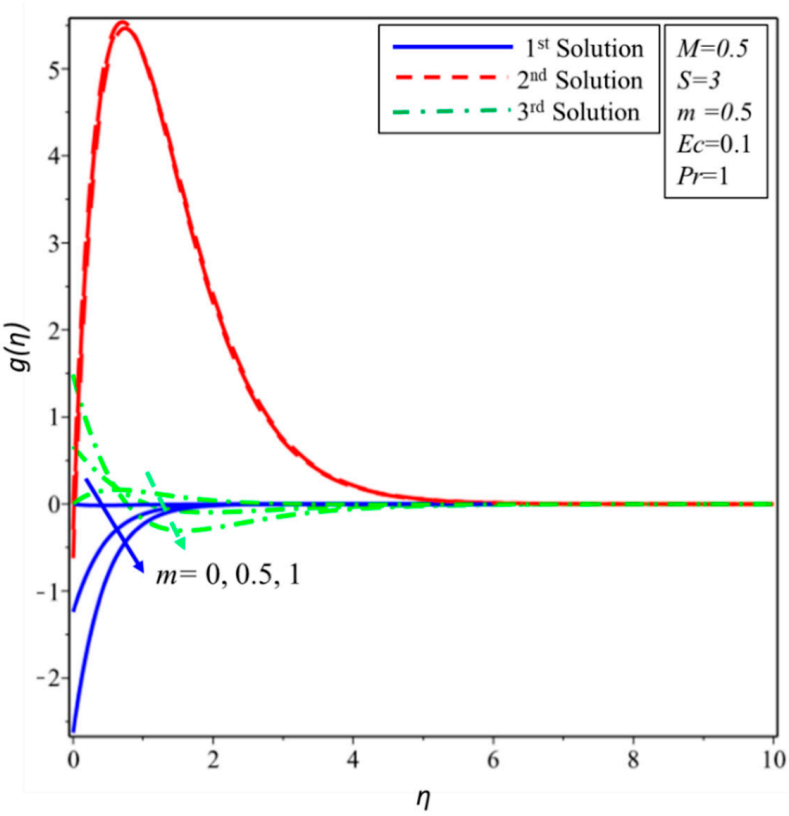


**Figure 10.** Angular velocity profile for different values of *m*.

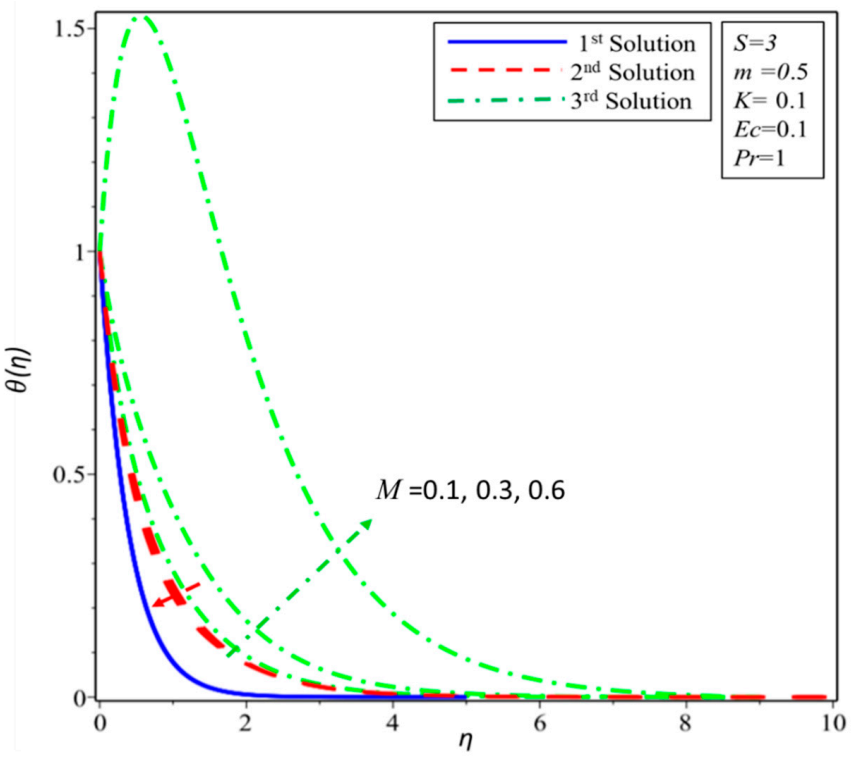


**Figure 11.** Temperature profile for different values of *m*.

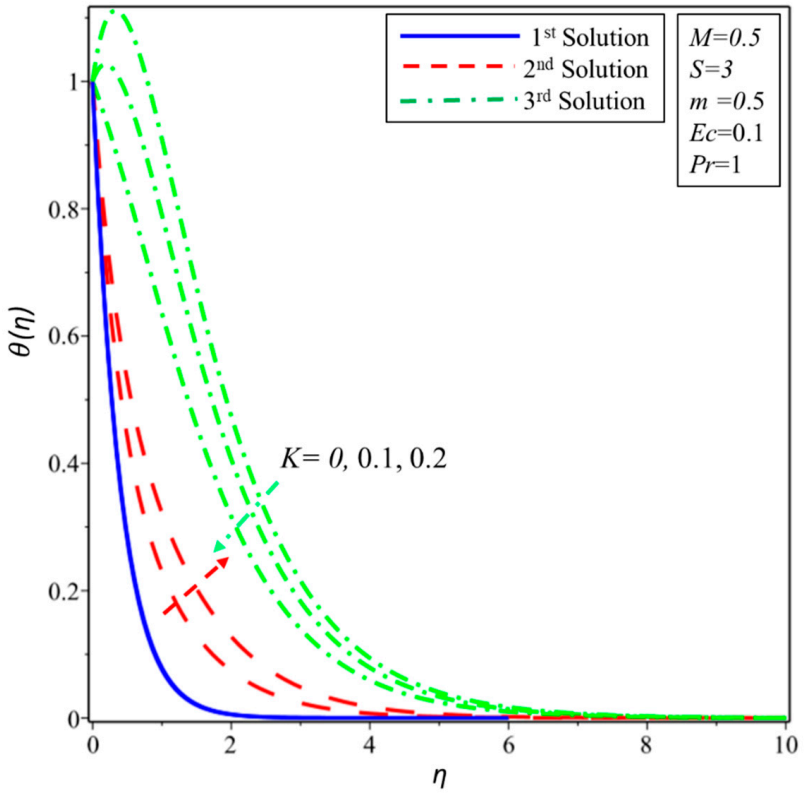


**Figure 12.** Temperature profile for different values of *K*.

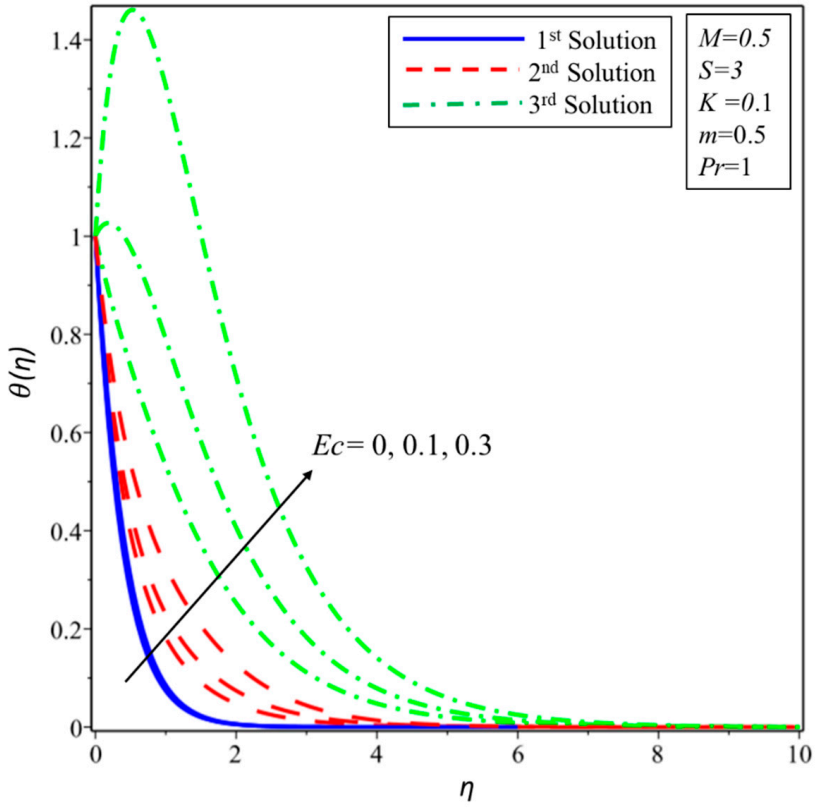


**Figure 13.** Temperature profile for different values of *Ec*.

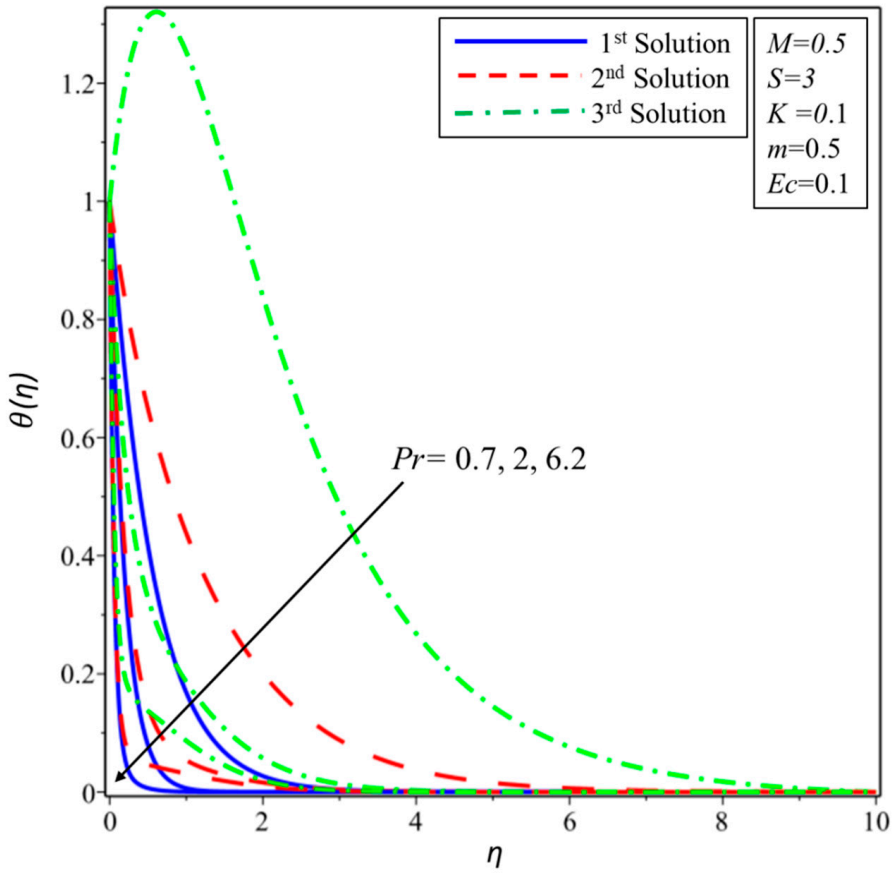


**Figure 14.** Temperature profile for different values of *Pr*.

Finally, Table 1 shows the values of the smallest eigenvalue. It is worth highlighting that the stability of solutions depends on the sign of the values of smallest eigenvalue $\varepsilon$. If the value of $\varepsilon$ is positive, then the initial growth of decay exists, and the flow becomes stable. Hence, the first solution is stable because the sign of $\varepsilon$ is positive. On the other hand, if the value of $\varepsilon$ is negative, then an initial growth of disturbance exists, and therefore the second and third solutions are said to be unstable.

**Table 1.** Smallest eigenvalues for different values of $K$ and $S$ when $M = 0.5$, $Pr = 1$, $m = 0.5$, and $Ec = 0.1$.

| | | $\varepsilon$ | | |
|---|---|---|---|---|
| ***K*** | ***S*** | **1st Solution** | **2nd Solution** | **3rd Solution** |
| 0.1 | 3 | 0.96439 | −0.78535 | −0.84652 |
| | 2.5 | 0.86425 | −0.60258 | −0.64035 |
| 0.2 | 3 | 0.88162 | −0.69025 | −0.72184 |
| | 3.7 | 0.61582 | −0.46325 | −0.52287 |

## 5. Conclusions

MHD flow of micropolar fluid over an exponential shrinking surface was addressed. Hartmann number, viscous dissipation, and Joule heating have been accounted for. Multiple solutions and stability analysis were the main objectives of this study. The shooting method was implemented to get the solutions and the three-stage Lobatto IIIA formula, developed in bvp4c with the help of finite difference code, was used to determine the stability of the solutions. The main points of this study are as follows:

1. Two solutions exist for the case of Newtonian fluid.
2. Three solutions exist for the case of no-Newtonian fluid in the specific values of the suction parameter.
3. Ranges of single and multiple solutions are dependent on the suction parameter.
4. Results of the stability analysis of solutions indicate that only the first solution is stable.
5. The thickness of the momentum boundary layer enhances in all solutions when the slip parameter is increased.
6. The thickness of the thermal boundary layer is directly proportional to the values of the Eckert number. As the Eckert number increases, the temperature of fluid also rises due to the high impact of the kinetic energy.
7. The occurrence of a higher velocity of the fluid is possible for unstable solutions when the magnetic parameter increases.
8. The thermal field has been noted as lower corresponding to a larger Prandtl number in all solutions.
9. The angular velocity of the micropolar fluid increased in the first and third solutions for the higher values of material and slip parameters.

**Author Contributions:** L.A.L. and J.R. derived the equations and generated the results. E.-S.M.S. and A.H.S. discussed the results. Z.O. and I.K. formulated the model and proof read the manuscript. All authors have read and agreed to the published version of the manuscript.

**Funding:** This research is funded by Researchers Supporting Project number (RSP-2019/33), King Saud University, Riyadh, Saudi Arabia.

**Acknowledgments:** Researchers Supporting Project number (RSP-2019/33), King Saud University, Riyadh, Saudi Arabia. This research is also supported by Universiti Utara Malaysia (UUM).

**Conflicts of Interest:** The authors declare no conflict of interest.

## References


1. Dero, S.; Rohni, A.M.; Saaban, A. MHD micropolar nanofluid flow over an exponentially stretching/shrinking surface: Triple solutions. *J. Adv. Res. Fluid Mech. Therm. Sci.* **2019**, *56*, 165–174.
2. Raza, J.; Liyanage, J.P.; Al Atat, H.; Lee, J. A comparative study of maintenance data classification based on neural networks, logistic regression and support vector machines. *J. Qual. Maint. Eng.* **2010**, *16*, 303–318. [CrossRef]
3. Raza, J.; Rohni, A.M.; Omar, Z. Rheology of micropolar fluid in a channel with changing walls: Investigation of multiple solutions. *J. Mol. Liq.* **2016**, *223*, 890–902. [CrossRef]
4. Khan, I.; Fatima, S.; Malik, M.Y.; Salahuddin, T. Exponentially varying viscosity of magnetohydrodynamic mixed convection Eyring-Powell nanofluid flow over an inclined surface. *Results Phys.* **2018**, *8*, 1194–1203. [CrossRef]
5. Jafarimoghaddam, A. On the Homotopy Analysis Method (HAM) and Homotopy Perturbation Method (HPM) for a nonlinearly stretching sheet flow of Eyring-Powell fluids. *Eng. Sci. Technol.* **2019**, *22*, 439–451. [CrossRef]
6. Kamran, M.; Wiwatanapataphee, B. Chemical reaction and Newtonian heating effects on steady convection flow of a micropolar fluid with second order slip at the boundary. *Eur. J. Mech.-B/Fluids* **2018**, *71*, 138–150. [CrossRef]
7. Beneš, M.; Pažanin, I.; Radulović, M. Rigorous derivation of the asymptotic model describing a nonsteady micropolar fluid flow through a thin pipe. *Comput. Math. Appl.* **2018**, *76*, 2035–2060. [CrossRef]
8. Kumar, M.S.; Sandeep, N.; Kumar, B.R. Three-dimensional magnetohydrodynamic rotating flow past a stretched surface with cross diffusion. *Chin. J. Phys.* **2017**, *55*, 2407–2421. [CrossRef]
9. Shah, Z.; Islam, S.; Ayaz, H.; Khan, S. Radiative heat and mass transfer analysis of micropolar nanofluid flow of Casson fluid between two rotating parallel plates with effects of Hall current. *J. Heat Transf.* **2019**, *141*, 022401. [CrossRef]
10. Khashi'ie, N.S.; Md Arifin, N.; Nazar, R.; Hafidzuddin, E.H.; Wahi, N.; Pop, I. Mixed Convective Flow and Heat Transfer of a Dual Stratified Micropolar Fluid Induced by a Permeable Stretching/Shrinking Sheet. *Entropy* **2019**, *21*, 1162. [CrossRef]
11. Bhattacharjee, B.; Chakraborti, P.; Choudhuri, K. Evaluation of the performance characteristics of double-layered porous micropolar fluid lubricated journal bearing. *Tribol. Int.* **2019**, *138*, 415–423. [CrossRef]
12. Lakshmi, R.V.; Sarojamma, G.; Sreelakshmi, K.; Vajravelu, K. Heat Transfer Analysis in a Micropolar Fluid with Non-Linear Thermal Radiation and Second-Order Velocity Slip. In *Applied Mathematics and Scientific Computing*; Birkhäuser: Cham, Switzerland, 2019; pp. 385–395.
13. Lund, L.A.; Omar, Z.; Khan, I. Mathematical analysis of magnetohydrodynamic (MHD) flow of micropolar nanofluid under buoyancy effects past a vertical shrinking surface: Dual solutions. *Heliyon* **2019**, *5*, e02432. [CrossRef] [PubMed]
14. Lund, L.A.; Omar, Z.; Khan, I. Steady incompressible magnetohydrodynamics Casson boundary layer flow past a permeable vertical and exponentially shrinking sheet: A stability analysis. *Heat Transf.* **2019**, *48*, 3538–3556. [CrossRef]
15. Uddin, M.S.; Bhattacharyya, K.; Shafie, S. Micropolar fluid flow and heat transfer over an exponentially permeable shrinking sheet. *Propuls. Power Res.* **2016**, *5*, 310–317.
16. Lund, L.A.; Ching, D.L.C.; Omar, Z.; Khan, I.; Nisar, K.S. Triple local similarity solutions of Darcy-Forchheimer Magnetohydrodynamic (MHD) flow of micropolar nanofluid over an exponential shrinking surface: Stability analysis. *Coatings* **2019**, *9*, 527. [CrossRef]
17. Mahanthesh, B.; Lorenzini, G.; Oudina, F.M.; Animasaun, I.L. Significance of exponential space-and thermal-dependent heat source effects on nanofluid flow due to radially elongated disk with Coriolis and Lorentz forces. *J. Therm. Anal. Calorim.* **2019**, 1–8. [CrossRef]
18. Lund, L.A.; Omar, Z.; Khan, I.; Dero, S. Multiple solutions of Cu-$C_6H_9NaO_7$ and Ag-$C_6H_9NaO_7$ nanofluids flow over nonlinear shrinking surface. *J. Cent. South Univ.* **2019**, *26*, 1283–1293. [CrossRef]
19. Ghosh, S.; Mukhopadhyay, S.; Vajravelu, K. Dual solutions of slip flow past a nonlinearly shrinking permeable sheet. *Alex. Eng. J.* **2016**, *55*, 1835–1840. [CrossRef]
20. Dero, S.; Uddin, M.J.; Rohni, A.M. Stefan blowing and slip effects on unsteady nanofluid transport past a shrinking sheet: Multiple solutions. *Heat Transf.* **2019**, *48*, 2047–2066. [CrossRef]

21. Dero, S.; Rohni, A.M.; Saaban, A.; Khan, I. Dual Solutions and Stability Analysis of Micropolar Nanofluid Flow with Slip Effect on Stretching/Shrinking Surfaces. *Energies* **2019**, *12*, 4529. [CrossRef]
22. Lund, L.A.; Omar, Z.; Khan, I.; Kadry, S.; Rho, S.; Mari, I.A.; Nisar, K.S. Effect of Viscous Dissipation in Heat Transfer of MHD Flow of Micropolar Fluid Partial Slip Conditions: Dual Solutions and Stability Analysis. *Energies* **2019**, *12*, 4617. [CrossRef]
23. Raza, J.; Rohni, A.M.; Omar, Z.; Awais, M. Rheology of the Cu-$H_2O$ nanofluid in porous channel with heat transfer: Multiple solutions. *Physica E* **2017**, *86*, 248–252. [CrossRef]
24. Mohanty, B.; Mishra, S.R.; Pattanayak, H.B. Numerical investigation on heat and mass transfer effect of micropolar fluid over a stretching sheet through porous media. *Alex. Eng. J.* **2015**, *54*, 223–232. [CrossRef]
25. Akbar, N.S.; Tripathi, D.; Khan, Z.H.; Bég, O.A. A numerical study of magnetohydrodynamic transport of nanofluids over a vertical stretching sheet with exponential temperature-dependent viscosity and buoyancy effects. *Chem. Phys. Lett.* **2016**, *661*, 20–30. [CrossRef]
26. Reddy, P.B.; Suneetha, S.; Reddy, N.B. Numerical study of magnetohydrodynamics (MHD) boundary layer slip flow of a Maxwell nanofluid over an exponentially stretching surface with convective boundary condition. *Propuls. Power Res.* **2017**, *6*, 259–268. [CrossRef]
27. Pal, D.; Biswas, S. Perturbation analysis of magnetohydrodynamics oscillatory flow on convective-radiative heat and mass transfer of micropolar fluid in a porous medium with chemical reaction. *Eng. Sci. Technol.* **2016**, *19*, 444–462. [CrossRef]
28. Salman Ahmed, N.J.; Khaleed, H.M.T.; Baig, M.A.A.; Khan, T.M.; Kamangar, S. Effect of viscous dissipation on aiding flow heat and mass transfer in porous cavity. In *American Institute of Physics Conference Series*; AIP: College Park, MD, USA, 2019; Volume 2104.
29. Rasool, G.; Zhang, T.; Shafiq, A.; Durur, H. Influence of chemical reaction on Marangoni convective flow of nanoliquid in the presence of Lorentz forces and thermal radiation: A numerical investigation. *J. Adv. Nanotechnol.* **2019**, *1*, 32. [CrossRef]
30. Hor, C.H.; Tso, C.P.; Chen, G.M. 4. Viscous Dissipation Effects in A Microchannel Caused by Oscillation of One Surface. *J. Eng. Technol. Appl. Phys.* **2019**, *1*, 13–17. [CrossRef]
31. Rasool, G.; Zhang, T.; Shafiq, A. Second grade nanofluidic flow past a convectively heated vertical Riga plate. *Phys. Scr.* **2019**, *94*, 125212. [CrossRef]
32. Raju, S.S.; Kumar, K.G.; Rahimi-Gorji, M.; Khan, I. Darcy–Forchheimer flow and heat transfer augmentation of a viscoelastic fluid over an incessant moving needle in the presence of viscous dissipation. *Microsyst. Technol.* **2019**, *25*, 3399–3405. [CrossRef]
33. Lund, L.A.; Omar, Z.; Khan, I.; Raza, J.; Bakouri, M.; Tlili, I. Stability Analysis of Darcy-Forchheimer Flow of Casson Type Nanofluid Over an Exponential Sheet: Investigation of Critical Points. *Symmetry* **2019**, *11*, 412. [CrossRef]
34. Adegbie, S.K.; Koriko, O.K.; Animasaun, I.L. Melting heat transfer effects on stagnation point flow of micropolar fluid with variable dynamic viscosity and thermal conductivity at constant vortex viscosity. *J. Niger. Math. Soc.* **2016**, *35*, 34–47. [CrossRef]
35. Waqas, M.; Farooq, M.; Khan, M.I.; Alsaedi, A.; Hayat, T.; Yasmeen, T. Magnetohydrodynamic (MHD) mixed convection flow of micropolar liquid due to nonlinear stretched sheet with convective condition. *Int. J. Heat Mass Transf.* **2016**, *102*, 766–772. [CrossRef]
36. Nadeem, U.S.; Khan, A.U. Stability analysis of Cu–$H_2O$ nanofluid over a curved stretching–shrinking sheet: Existence of dual solutions. *Can. J. Phys.* **2019**, *97*, 911–922.
37. Lund, L.A.; Omar, Z.; Khan, I. Quadruple solutions of mixed convection flow of magnetohydrodynamic nanofluid over exponentially vertical shrinking and stretching surfaces: Stability analysis. *Comput. Methods Programs Biomed.* **2019**, *182*, 105044. [CrossRef]
38. Rahman, M.M.; Rosca, A.V.; Pop, I. Boundary layer flow of a nanofluid past a permeable exponentially shrinking surface with convective boundary condition using Buongiorno's model. *Int. J. Numer. Methods Heat Fluid Flow* **2015**, *25*, 299–319. [CrossRef]
39. Harris, S.D.; Ingham, D.B.; Pop, I. Mixed convection boundary-layer flow near the stagnation point on a vertical surface in a porous medium: Brinkman model with slip. *Transp. Porous Media* **2009**, *77*, 267–285. [CrossRef]

40. Lund, L.A.; Omar, Z.; Khan, I.; Seikh, A.H.; Sherif ES, M.; Nisar, K.S. Stability analysis and multiple solution of Cu–$Al_2O_3$/$H_2O$ nanofluid contains hybrid nanomaterials over a shrinking surface in the presence of viscous dissipation. *J. Mater. Res. Technol.* **2019**. [CrossRef]
41. Waini, I.; Ishak, A.; Pop, I. Transpiration effects on hybrid nanofluid flow and heat transfer over a stretching/shrinking sheet with uniform shear flow. *Alex. Eng. J.* **2019**. [CrossRef]